

AN ULTRA-BROADBAND, COPLANAR-WAVEGUIDE FED CIRCULAR MONOPOLE ANTENNA WITH IMPROVED RADIATION CHARACTERISTICS

N.-W. Chen and Y.-C. Liang

Department of Electrical Engineering
National Central University
No. 300 Jungda Rd., Jhongli 32004, Taiwan

Abstract—A planar, circular monopole antenna (PCMA) with satisfactory radiation characteristics over an ultra-broadband is demonstrated. Compared to the classical coplanar-waveguide (CPW) fed PCMA, the radiation characteristics of the proposed CPW-fed PCMA are significantly improved, particularly at the frequencies around the higher band edge. This improvement is achieved by exploiting a tapered and periodically corrugated edge design to the CPW ground plane. The tapered and corrugated ground-plane edge design, in essence, modifies the current distribution on the circular disc as well as along the edges of the ground plane. With this design, the cross polarization radiation is remarkably reduced, and the pattern deterioration, especially at the planes perpendicular to the plane of the antenna, is greatly alleviated. The demonstrated CPW-fed PCMA features an over 150% VSWR = 2 fractional bandwidth (0.81–5.87 GHz) and promises satisfactory radiation characteristics over the entire band. The proposed PCMA is poised for applications in wideband/ultra-wideband communication systems.

1. INTRODUCTION

Owing to the proliferation of broadband wireless communication systems, there is an increasing demand for wideband antennas, especially for those poised to operate in the microwave regime. Technically speaking, the planar, traveling-wave type antennas, such as the tapered-slot antennas [1–4], appear to be a commonly considered candidate for the antennas of this sort and have been studied

Corresponding author: N.-W. Chen (nwchen@ee.ncu.edu.tw).

extensively in the past. A general discussion of their designs and applications is provided in [5, 6] and the references therein. However, the large electrical dimensions in nature often render this type of antennas unsuitable for applications in personal mobile devices. Recently, the design of relatively compact, planar monopole antennas based on the microstrip structures has been reported [7–12] to meet the bandwidth requirement. Indeed, compared to the classical (wire) monopole antennas, the planar monopole antennas are of a significantly wider bandwidth and have similar radiation characteristics at the lower frequencies of the band. However, the radiation characteristics deteriorate at the frequencies in the vicinity of the higher band edge. As pointed out in [10, 12], at these frequencies, the radiation patterns especially at the principle planes perpendicular to the antenna plane deteriorate because of the excitation of the higher-mode currents on the antenna structure as well as the enhanced edge currents on the ground plane. More specifically, at the E -plane perpendicular to the antenna plane, the field intensity becomes weaker along the antenna axis. Also, at the H -plane, the nulls start emerging at the broadside of the radiation pattern and the pattern, hence, becomes less omnidirectional.

In this paper, a planar, circular monopole antenna (PCMA) fed by a coplanar waveguide (CPW) is proposed to promise the aforementioned impedance bandwidth together with satisfactory radiation characteristics through the whole band. Antennas of this sort have been proposed previously [13–16]. Technically speaking, the CPW-fed PCMA exploits the CPW configuration to permit easy integration with the uniplanar monolithic integrated circuits/monolithic microwave integrated circuits. However, similar deterioration of the radiation characteristics at the frequencies close to the higher band edge renders the antenna inapplicable at these frequencies. Again, the higher-mode currents on the circular disc and the enhancement of the ground-plane edge currents around the feed are the primary reasons for the deterioration. This paper aims to resolve this issue by employing modifications on the antenna ground-plane. It is shown that the demonstrated CPW-fed PCMA features satisfactory radiation patterns over the whole band via a tapered and periodically corrugated edge structure on the ground plane. With the ground-plane modifications, the aforementioned pattern deterioration is greatly alleviated. In addition, the cross-polarization radiation at the principle planes perpendicular to the antenna plane is significantly reduced. The demonstrated antenna is of an over 150% VSWR = 2 bandwidth (0.81–5.87 GHz) and of satisfactory radiation patterns at all principal planes over the entire band.

2. ANTENNA STRUCTURE AND ANALYSIS

In this section, the design and analysis of the proposed CPW-fed PCMA depicted in Fig. 1(a) are presented to demonstrate the improvement regarding the impedance bandwidth and radiation characteristics. For comparison, the corresponding *classical* CPW-fed PCMA reported in [13] is presented in Fig. 1(b). As shown in Figs. 1(a) and (b), the PCMA features a circular disc monopole imprinted on a dielectric substrate of thickness 1.524 mm, $\epsilon_r = 3.48$, and $\tan \delta = 0.005$. The circular monopole is fed through a 50 Ω CPW. The dimensions of the two antenna structures are presented in the table of Fig. 1. The antennas are characterized using the in-house time-domain integral-equation based solver [17], and the simulation results are compared to the measurement ones for design verification.

In Fig. 1(a), the configuration of the proposed CPW-fed PCMA antenna essentially has its basis in the *classical* PMCA (Fig. 1(b))

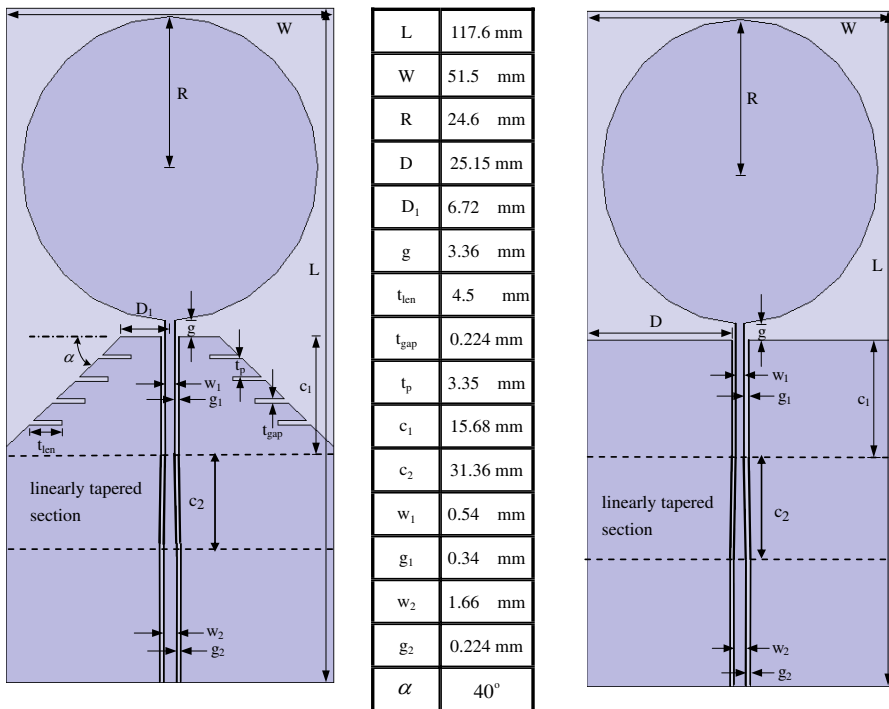


Figure 1. Configuration and dimensions of (a) the proposed PCMA and (b) the classical PCMA.

proposed in [13]. The detailed design criteria and characteristics of the classical PMCA can be found therein. Technically speaking, compared to the classical PMCA, the proposed CPW-fed PCMA exploits a tapered and periodically corrugated ground plane for improvement on the bandwidth together with the radiation characteristics. In what follows, the characteristics of the classical PMCA are first outlined, and the design and analysis of the proposed PCMA regarding the improvement on the impedance bandwidth and radiation characteristics of the classical PCMA are then described.

Theoretically speaking, the broad bandwidth of the classical PMCA is attributed to the multi-resonant characteristic of the circular disc structure, and the first resonant frequency of the classical PMCA is predominately determined by the radius of the circular disc [13].

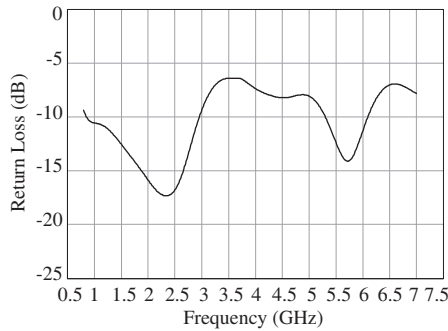


Figure 2. Return loss of the classical PCMA.

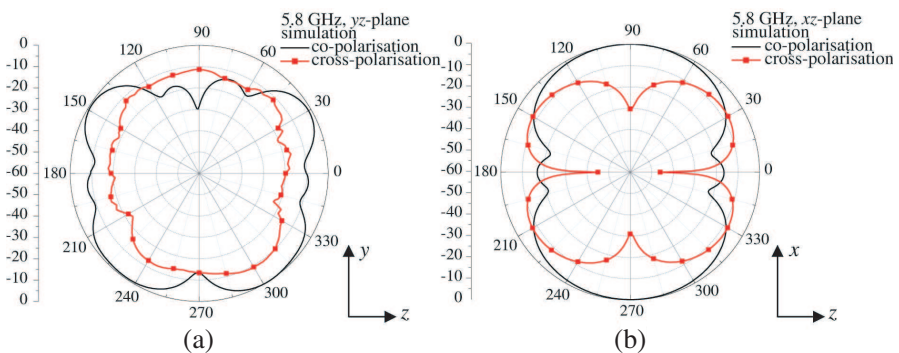


Figure 3. Normalized co-polarization (black line) and cross-polarization (red line with square markers) radiation patterns of the classical PCMA at (a) yz -plane and (b) xz -plane at $f = 5.8$ GHz.

On the other hand, the gap between the circular disc and the CPW feed, denoted as g in Figs. 1(a) and (b), has been shown to be a key parameter that affects the PCMA impedance bandwidth. Indeed, the increase and decrease of g respectively enhances and weakens the capacitive coupling between the circular disc and the ground plane, which appears to predominately affect the resonant frequencies of the circular disc. Here, the dimensions R and g are chosen to ensure the first resonant frequency of the proposed PCMA is at about 2.4 GHz, as shown in Fig. 2. With this choice, the lower 10-dB cutoff frequency of the classical PCMA is 0.78 GHz, and the return loss at the frequencies between 0.78 GHz and 3 GHz, as well as 5.3 GHz and 6.1 GHz is greater than 10 dB. As for the radiation patterns, the patterns at the lower frequencies of the band, in essence, are similar to the patterns of a classical quarter-wavelength (wire) monopole, but the patterns start deteriorating at higher frequencies as demonstrated in Figs. 3(a) and (b). As shown in Fig. 3(a), at $f = 5.8$ GHz, the yz -plane pattern becomes asymmetric with respect to the z -axis, and the field intensity becomes weaker along the y -direction. Furthermore, in Fig. 3(b), the xz -plane pattern becomes less isotropic and the nulls are observed along the z -direction. On the other hand, the cross-polarization level at the yz - and xz -planes drastically decreases. It appears that the enhancement of the edge currents around the feed is primarily responsible for the high cross-polarization radiation. The current distributions on the classical PCMA at the frequency $f = 5.8$ and 0.8 GHz are shown in Figs. 4(a) and (b), respectively. It is

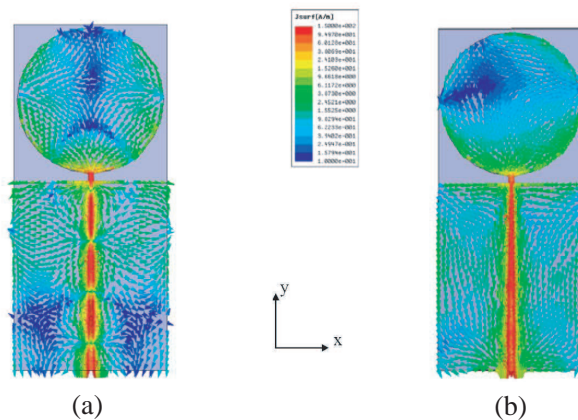


Figure 4. Current flow on the surface of the classical PCMA at (a) 5.8 GHz and (b) 0.8 GHz.

clearly seen that, at the higher frequency, the horizontal (x -direction) current flow on the ground plane is enhanced. To further improve the impedance bandwidth as well as the radiation characteristics of the classical PCMA, two modifications employed on the ground plane are proposed herein and described as follows.

First, regarding the bandwidth, it has been shown that the tapered ground plane design [16] appears to be an effective means of increasing the bandwidth. Here, the ground plane with linear tapered edges around the CPW feed is adopted herein for the proposed CPW-fed PCMA (Fig. 1(a)). The linear taper edges are configured with the angle α and the length D_1 as depicted in Fig. 1(a). It appears that α is the key parameter that affects the characteristics of the PCMA. The corresponding return loss, real part of the input impedance, and imaginary part of the input impedance, are shown in Fig. 5.

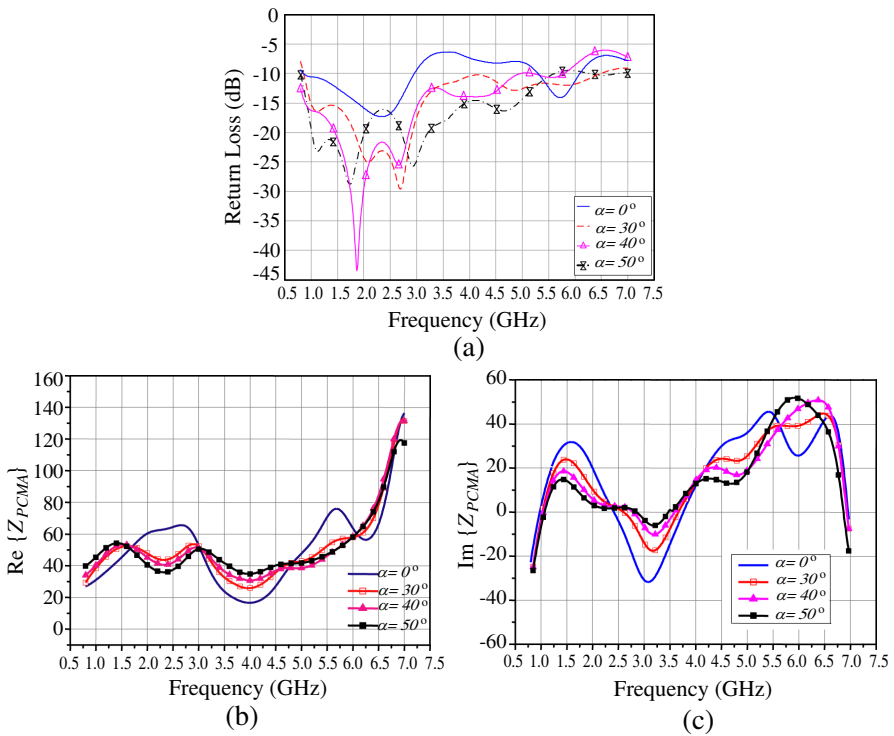


Figure 5. (a) Return loss of the classical PCMA with a tapered ground plane with different α , (b) real part of the input impedance of the classical PCMA with a tapered ground plane with different α , (c) imaginary part of the input impedance of the classical PCMA with a tapered ground plane with different α .

and imaginary part of the input impedance of the classical PCMA with a tapered ground plane of different α compared against the one without this modification ($\alpha = 0$) are demonstrated in Figs. 5(a), (b), and (c), respectively. As shown in Figs. 5(b) and (c), the tapered ground plane, in essence, leads to a relatively moderate variation of the input impedance over the whole band when compared to the one without this modification. Here, $\alpha = 40^\circ$ is used and, with this choice, the return loss at the frequencies ranging from 0.78 to 6.0 GHz is greater than 10 dB. On the other hand, the radiation characteristics at the frequencies close to the higher band edge are improved. As demonstrated in Fig. 6, at $f = 5.8$ GHz, the xz -plane pattern is rendered more isotropic since the nulls observed with the classical PCMA are eliminated. In addition, at the yz -plane, the cross-polarization level (Table 1) and the field intensity along the y -axis

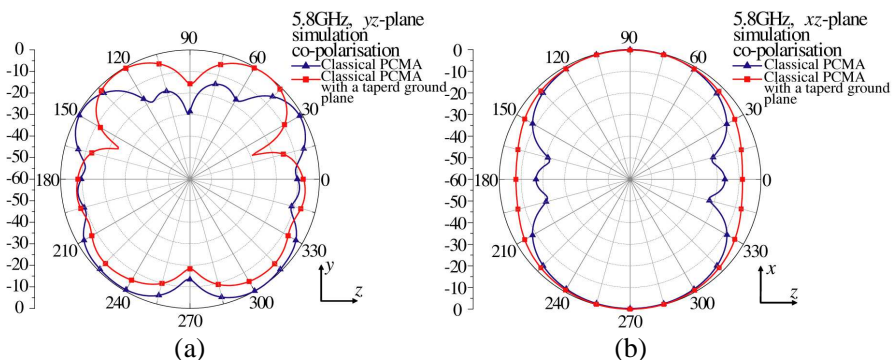


Figure 6. The radiation patterns of the classical PCMA (blue line) and the classical PCMA with a tapered ground plane (red line) at (a) yz -plane and (b) xz -plane.

Table 1. Simulated cross-polarization level of the classical PCMA, the classical PCMA with tapered edges, and the proposed PCMA at different frequencies (unit: dB).

Frequency	0.9 GHz			1.8 GHz			2.4 GHz			5.8 GHz		
Principal Cut	xy	yz	xz									
Classical PCMA	17.4	10.9	9.7	18.3	21.9	16.3	23.9	31.4	26.5	21.6	9.2	7.3
Classical PCMA with tapered edges	14.6	8.9	7.4	21.2	25.6	20.9	24	32	25.9	19.4	13.4	11
Proposed PCMA	19	11.6	13.4	20.7	23.6	17.4	24.4	33.1	26.3	19.2	14.3	10.4

are increased. The improvement on the above-mentioned radiation characteristics is mainly attributed to the reduction of the horizontal current, i.e., the x -component of the current flow, along the ground-plane edges in the vicinity of the CPW feed via the tapered edge design (Fig. 7(a)). However, this design renders the cross-polarization level at the frequencies close to the lower band edge dropped (Table 1). As demonstrated in Fig. 7(b), at $f = 0.9$ GHz, it appears that the current flow along the tapered edges is relatively enhanced, which leads to an increase of the cross-polarization radiation. Hence, a decrease of the cross-polarization level at yz - and xz -planes is observed.

To tackle the aforementioned issue of poor cross-polarization level at the lower frequencies of the band, the periodic corrugated structures are employed on the tapered edges of the ground plane. As depicted in Fig. 1(a), the corrugated structures are configured with the dimensions t_{len} , t_{gap} , and t_p . Technically speaking, the corrugated-edge structures essentially aim to redirect the current flow along the ground-plane edges close to the CPW feed so that the cross-polarization from them is reduced. As shown in Fig. 8, with this structure, the current flow along the two sides of each groove is in the opposite direction, and therefore the unfavorable cross-polarization radiation from the edge currents appears to be greatly reduced. On the other hand, with the corrugated edges, it appears that the impedance matching between the CPW feed and the circular-disc structures is relatively improved at the frequencies close to the lower band edge. Specially, the parameter t_{len} is shown to have the key impact on the antenna input impedance. According to the current plot on the antenna plane at $f = 0.9$ GHz shown in Fig. 9, it is obvious that the intensity of the current on the

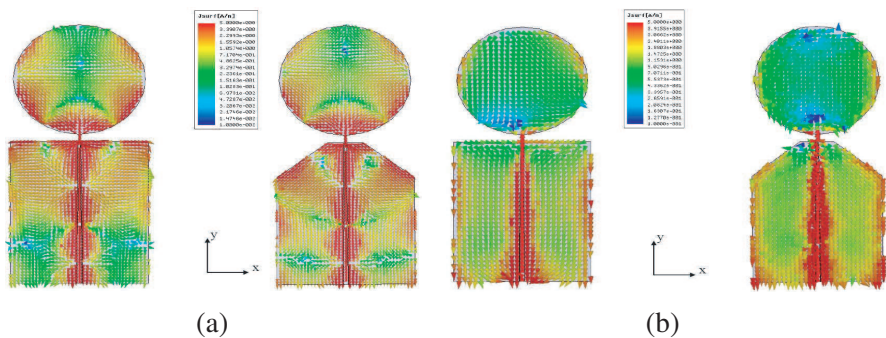


Figure 7. Comparison of the current intensity of the classical PCMA (left) and the classical PCMA with a tapered ground plane (right) at (a) $f = 5.8$ GHz and (b) $f = 0.9$ GHz.

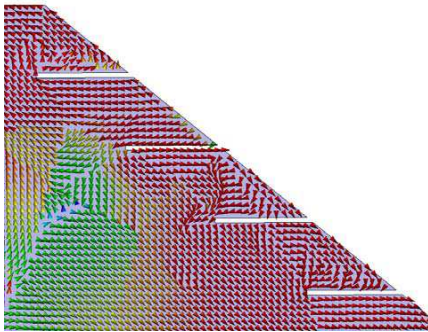


Figure 8. Current flow in the vicinity of the corrugated edges.

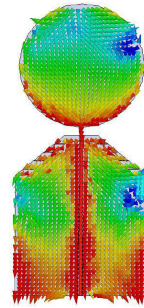
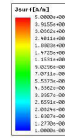


Figure 9. Current flow on the proposed PCMA at $f = 0.9$ GHz.

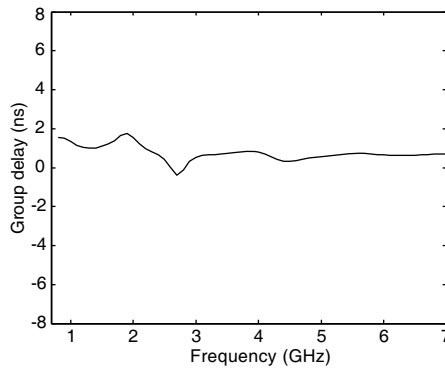


Figure 10. Simulated group delay of the proposed PCMA.

circular disc greatly increases, and the current distribution becomes more symmetric with respect to the antenna axis when compared to the one of the classical PCMA shown in Fig. 4(b). As a consequence, the radiation characteristics are improved. On the other hand, the simulated group delay of the proposed PCMA is demonstrated in Fig. 10. A flat variation (2 ns) of the group delay over the entire operation band is observed.

3. ANTENNA MEASUREMENT

The proposed PCMA is fabricated on a Rogers 4350B substrate of the same parameters used in the aforementioned analysis for design verification. The photograph of the fabricated PCMA is demonstrated

in the inset of Fig. 11. The measured return loss and radiation patterns compared against the simulation ones are shown in Figs. 11 and 12, respectively. The corresponding measured cross-polarization level compared to the simulated one is listed in Table 2. In Fig. 11, the measured and simulated return loss are in good agreement, especially at the lower frequencies of the band. The measured 10-dB lower and higher cutoff frequencies are, respectively, 0.81 GHz and 5.87 GHz, and the corresponding fractional bandwidth is over 150%. It appears that the measured bandwidth is slightly less than the simulated one (0.75–5.9 GHz), which is possibly owing to the parasitic effect of the SMA connector.

The measured radiation patterns compared with the simulated ones at $f = 0.9, 2.4,$ and 5.8 GHz are demonstrated in Figs. 12(a), (b), and (c), respectively. It is shown that the measured co-polarization and cross-polarization patterns are in very good agreement with the simulated ones over the entire band. In addition, the measured patterns show that the deterioration of the patterns at the frequency (5.8 GHz) of the higher band edge observed for the classical PCMA is greatly alleviated. More specifically, the measured cross-polarization level of the classical PCMA, the classical PCMA with a tapered ground plane, and the classical PCMA with a tapered and corrugated ground plane are listed in Table 2. As listed in Table 2, the cross-polarization level of the proposed PCMA is significantly improved at the frequency (900 MHz) of the lower band edge.

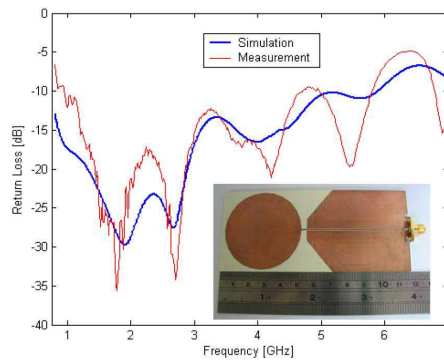
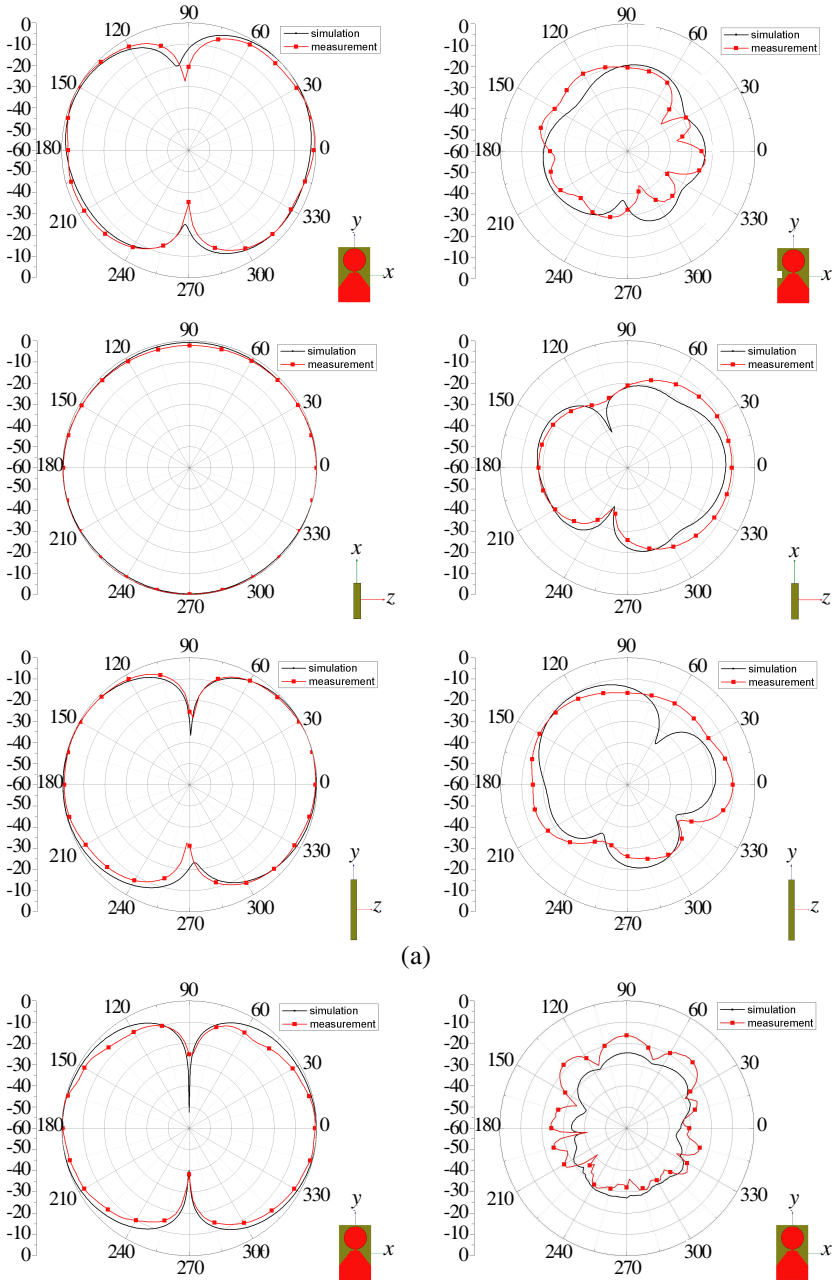
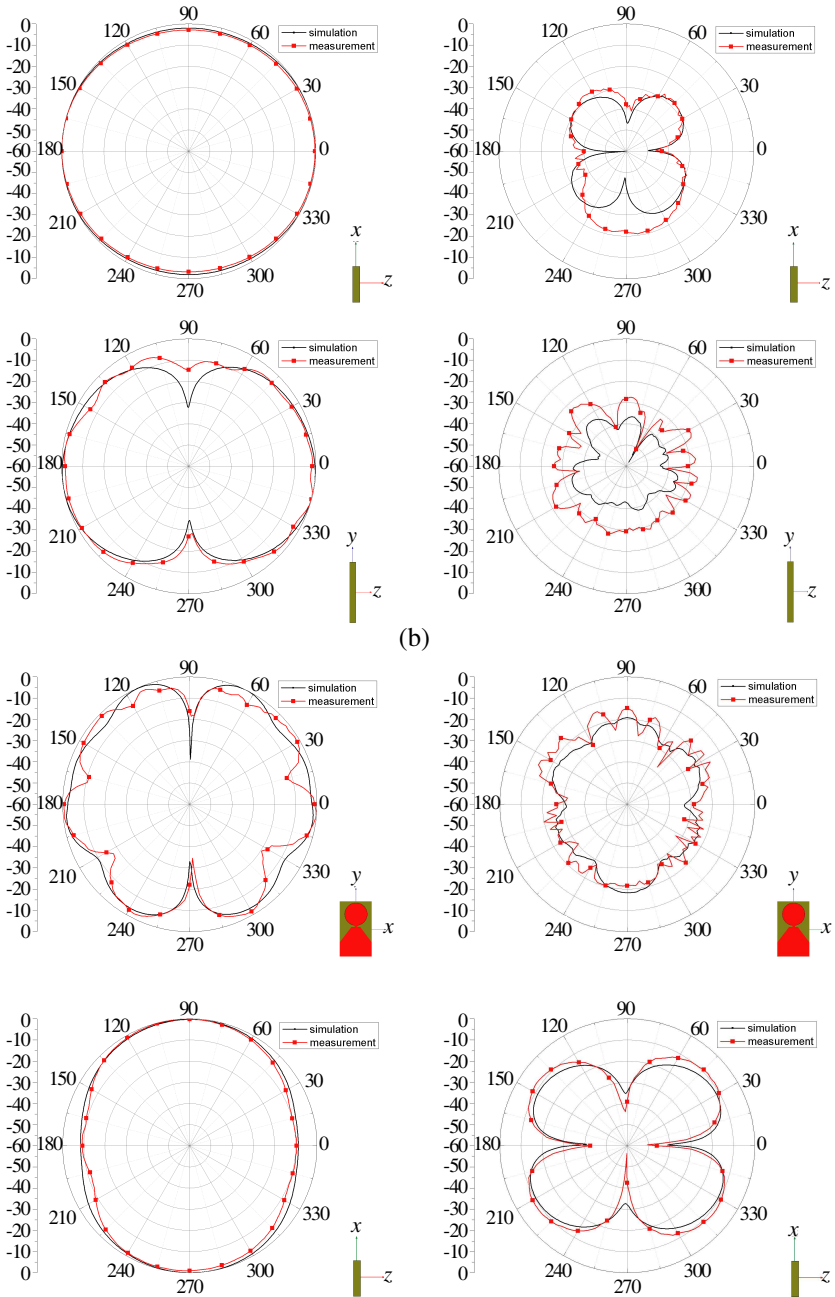


Figure 11. Photograph of the fabricated PCMA together with the measured and simulated return loss of the proposed PCMA.





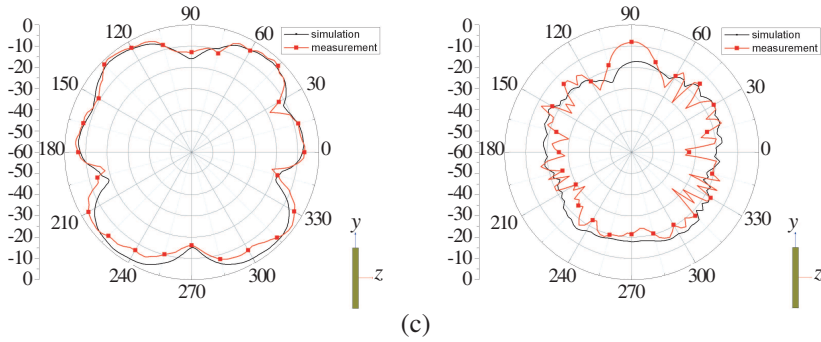


Figure 12. Measured and simulated normalized co-polarization (left panel) and cross-polarization (right panel) patterns at (a) $f = 0.9$ GHz, (b) $f = 2.4$ GHz, and (c) $f = 5.8$ GHz.

Table 2. Measured cross-polarization level of the classical PCMA, the classical PCMA with tapered edges, and the proposed PCMA at different frequencies (unit: dB).

Frequency	0.9 GHz			1.8 GHz			2.4 GHz			5.8 GHz		
	xy	yz	xz	xy	yz	xz	xy	yz	xz	xy	yz	xz
Principal Cut												
Classical PCMA	17	11.2	10.4	13.9	21	15.3	15.8	21.5	22.6	15.5	3.8	8.2
Classical PCMA with tapered edges	16	9.6	8.5	14	22.1	18.4	15.5	21.4	19.1	14.4	6.5	8.3
Proposed PCMA	17.5	11.4	11.2	14.2	21	16.8	15.4	21.2	21	14.3	7.8	8

4. CONCLUSION

An ultra-broadband, CPW-fed PCMA is demonstrated. The proposed PCMA features a 150% $VSWR = 2$ fractional bandwidth, a relatively compact size, and satisfactory radiation characteristics over the entire band. Indeed, compared to the classical PCMA, the radiation characteristics are significantly improved with a tapered and corrugated ground-plane design. The proposed PCMA is expected to find applications in wideband/ultra-wideband communication systems as a transceiver antenna.

REFERENCES

1. Yngvesson, K. S., D. H. Schaubert, T. L. Korzeniowski, E. L. Kolberg, T. Thungren, and J. F. Johansson, "Endfire tapered slot antennas on dielectric substrate," *IEEE Trans. Antennas and Propagat.*, Vol. 33, No. 12, 1392–1400, Dec. 1985.
2. Yngvesson, K. S., T. L. Korzeniowski, Y.-S. Kim, E. L. Kolberg, and J. F. Johansson, "The tapered slot antenna — A newintegrated element for millimeter-wave applications," *IEEE Trans. Microw. Theory Technol.*, Vol. 37, No. 2, 365–374, Feb. 1989.
3. Muldavin, J. B. and G. M. Rebeiz, "Millimeter-wave tapered slot antenna on synthesized low permittivity substrates," *IEEE Trans. Antennas and Propagat.*, Vol. 47, No. 8, 1276–1280, Aug. 1999.
4. Chen, N.-W., C.-T. Chuang, and J.-W. Shi, "A W-band linear tapered slot antenna on rectangular-grooved silicon substrate," *IEEE Antennas and Wireless Propagat. Lett.*, Vol. 6, 90–92, 2007.
5. Balanis, C. A., *Antenna Theory: Analysis and Design*, 2nd Edition, John Wiley & Sons, 1997.
6. Kraus, J. D. and R. J. Marhefka, *Antennas: For All Applications*, 3rd Edition, McGraw-Hill, 2002.
7. Agrawall, N. P., G. Kumar, and K. P. Ray, "Wide-band planar monopole antennas," *IEEE Trans. Antennas and Propagat.*, Vol. 46, No. 2, 294–295, 1998.
8. Ammann, M. J. and Z. N. Chen, "Wideband monopole antennas for multi-band wireless systems," *IEEE Antennas Propag. Mag.*, Vol. 45, No. 2, 146–150, Apr. 2003.
9. Antonino-Daviu, E., M. Cabedo-Fabre's, M. Ferrando-Bataller, and A. Valero-Nogueira, "Wideband double-fed planar monopole antennas," *Electron. Lett.*, Vol. 39, No. 23, 1635–1636, Nov. 2003.
10. Liang, J., C. C. Chiau, X. Chen, and C. G. Parini, "Study of a printed circular disc monopole antenna for UWB applications," *IEEE Trans. Antennas and Propagat.*, Vol. 53, No. 11, 3500–3504, 2005.
11. Liang, J., C. C. Chiau, X. Chen, and C. G. Parini, "Printed circular disc monopole antenna for ultra-wideband applications," *Electron. Lett.*, Vol. 40, No. 20, 1246–1247, 2004.
12. Azenui, N. C. and H. Y. D. Yang, "A printed crescent patch antenna for ultrawideband applications," *IEEE Antennas and Wireless Propagat. Lett.*, Vol. 6, 113–116, 2007.
13. Liang, J., L. Guo, C. C. Chiau, X. Chen, and C. G. Parini, "Study

- of CPW-fed circular disc monopole antenna for ultrawideband applications,” *IEE Proceedings Microwaves Antennas and Propagation*, Vol. 152, No. 6, 520–526, 2005.
14. Chung, K., T. Yun, and J. Choi, “Wideband CPW-fed monopole antenna with parasitic elements and slots,” *Electron. Lett.*, Vol. 40, No. 17, 1038–1040, 2004.
 15. Wang, W., S.-S. Zhong, and S.-B. Chang, “A novel wideband coplanar-fed monopole antenna,” *Microwave Opt. Tech. Lett.*, Vol. 43, 50–52, 2004.
 16. Wu, Q., R. Jin, J. Geng, and M. Ding, “Compact CPW-fed quasi-circular monopole with very wide bandwidth,” *Electron. Lett.*, Vol. 43, 69–70, 2007.
 17. Chen, N.-W., “A Magnetic frill source model for time-domain integral-equation based solvers,” *IEEE Trans. Antennas and Propagat.*, Vol. 55, 3093–3098, Nov. 2007.